Specific rate constants k(E,J) for the dissociation of NO 2 . I. Time-resolved study of rotational dependencies

B. Abel, B. Kirmse, J. Troe, and D. Schwarzer

Citation: The Journal of Chemical Physics **115**, 6522 (2001); doi: 10.1063/1.1398305
View online: http://dx.doi.org/10.1063/1.1398305
View Table of Contents: http://scitation.aip.org/content/aip/journal/jcp/115/14?ver=pdfcov
Published by the AIP Publishing

Specific rate constants $k(E,J)$ for the dissociation of NO_2. I. Time-resolved study of rotational dependencies

B. Abel,[a] B. Kirmse, and J. Troe
Institut für Physikalische Chemie, Universität Göttingen, Tammannstrasse 6, D-37077 Göttingen, Germany

D. Schwarzer
Max-Planck-Institut für biophysikalische Chemie, Am Fassberg 11, D-37077 Göttingen, Germany

(Received 22 January 2001; accepted 9 July 2001)

The effect of rotational excitation on the specific rate constants $k(E,J)$ of the unimolecular decomposion of NO_2 has been investigated. Time-resolved pump- and probe experiments with sub-ps time resolution are reported in which NO_2 molecules with well-defined rotational and vibrational energy distributions were optically excited near and above the dissociation threshold. The subsequent unimolecular decay of the reacting NO_2 molecules was probed by time-resolved laser-induced fluorescence of the disappearing NO_2 via excitation to Rydberg states. At constant photolysis wavelength, increasing rotational energy (up to 310 cm^{-1}) was found to leave the overall decay rate nearly unaffected. This observation can be rationalized by assuming a compensation of the angular momentum and energy dependences of the specific rate constants when J and E are changed at the same time. Keeping the total energy E nearly constant and changing J independently, the effect of rotation on the decay rate can be separated and observed more clearly. From the experimental data we conclude that, for sufficiently high J and constant total energy, molecules with larger J dissociate more slowly than molecules with small J, which is in agreement with predictions from statistical unimolecular rate theory. © *2001 American Institute of Physics.*
[DOI: 10.1063/1.1398305]

I. INTRODUCTION

The unimolecular dissociation/recombination reaction $NO_2 \Leftrightarrow O+NO$ has played an important role in the development of unimolecular rate theory. Early studies of the pressure dependence of the thermal unimolecular dissociation/recombination reaction and of the wavelength dependence of Stern–Volmer plots for photolysis quenching led to first estimates of the specific rate constants $k(E)$ of dissociation.[1–4] Although being indirect and only derived by calibration against collision frequencies, the specific rate constants appeared to follow the predictions from statistical unimolecular rate theory.[5,6] At the same time, first photofragment spectra of NO_2 photolysis were obtained[7,8] which, however, were more difficult to reconcile with statistical unimolecular rate theory.[5,6,9]

It is not surprising that NO_2 dissociation studies experienced a renaissance when direct state- and time-resolving experimental techniques became available. The question arose whether the earlier conclusions about statistical behavior of the unimolecular dissociation would still hold on a more detailed level. A number of groups determined kinetic energy distributions of the fragments,[10] product state distributions,[11,12] photofragment excitation spectra,[13,14] zero kinetic energy photo-fragment spectra,[15] transient grating spectra,[16,17] and double resonance spectra of excited NO_2 close to the dissociation threshold.[18] Picosecond pump-and-probe photofragment spectroscopy allowed for a time-resolved investigation of the dissociation dynamics of NO_2.[19–23] At energies high above the dissociation threshold, the lifetime of excited NO_2 is faster than the rotational period, such that information about excited-state dynamics could also be obtained from measurements of product angular distributions and of alignments of the rotational angular momentum with respect to the fragment recoil velocity.[24]

The large number of experimental observations makes NO_2 an attractive system for examining theoretical models. Potential energy surfaces (PES) have been calculated on various levels of accuracy.[25–30] In addition to statistical calculations on parametrized potentials,[6,9] and *ab initio* PES's,[27,31–33] also full 3-D quantum mechanical calculations of resonance spectra were reported for $J=0$.[33] The conclusion from the earliest work,[6,9] that near-statistical behavior can be assumed for NO_2 *on average*, was confirmed in the recent experimental and theoretical studies. However, on a more state-resolved level, a variety of complications arise. Experimental, as well as theoretical work, provides evidence for more state-specific properties of the dissociation rate beyond the E- and J-dependence accounted for by statistical theories. On a microscopic level, the dissociation appears to be inherently related to specific resonance states whose widths show fluctuations around average values which, however, are related to the specific rate constants from statistical theories (for more details see Refs. 31–34).

Besides the general question of near-statistical or non-statistical behavior, the influence of rotation on the dissociation rate is of interest.[35–37] One asks again whether the rota-

[a]Author to whom correspondence should be addressed. Electronic mail: babel@gwdg.de

tional dependence of the specific rate constants follows statistical predictions or is of different character.[38,39] Much work has been done on the quantum yield of photodissociation at wavelengths larger than the photodissociation threshold. It was shown that rotational energy of the molecule is available for the dissociation process.[2–4,14,40,41] These findings, however, do not provide quantitative information about the rates of rotationally excited molecules in comparison to nonrotating molecules.

At present, a large body of data is available for the photodissociation of jet-cooled (almost) nonrotating NO_2 molecules, while much less is known about the dependence of the dissociation rates on rotation. There are two alternatives for studying the effects of rotation in the time domain: Time-resolved double-resonance experiments with state-resolution or time-resolved experiments with well-characterized rovibrational ensembles distributions. Time-resolved double-resonance ps pump-and-probe spectroscopy was recently applied by Wittig and co-workers.[22,23] A series of rotationally resolved decomposition experiments with time-resolved detection of the forming NO was made, in which J was varied, while the quantum number K was kept close to zero. Infrared pre-excitation of NO_2 was achieved by employing a high resolution optical parametric oscillator for pre-excitation prior to ps-excitation and subsequent decomposition of the molecules. With this technique the rotational quantum number of dissociating molecules was well-defined without, however, being able to have full energy resolution of the excited molecules. In addition, the range of accessible J- and K-values was limited for experimental reasons. It was found that the dependence of the dissociation rates on J is small in the investigated range of J- and K-values, which was attributed to full or partial conservation of the projection of J onto the molecular axis, i.e., to K-conservation.

In the present article we describe an alternative experimental approach in which we study rotational effects by monitoring the decay of well-defined broader rotational distributions of NO_2 in time-resolved subpicosecond experiments. The rotational temperatures in the experiments of this work were characterized spectroscopically. Although complete J-resolution was sacrificed, a broad range of J- and K-values could be accessed such that larger effects of molecular rotation on the lifetimes could be detected. The extension of the range beyond that accessible in Ref. 23 appeared important because only small effects were detected over the range of J-values between 1 and 15 at $K=0$.[23] In addition, it appeared of interest to measure the decay of the parent NO_2 molecules instead of the formation of the product NO. In this way multi-exponential decays of NO_2 could be identified over a broad range of rotational energies, total energies, and excitation energies which was not possible in Refs. 22 and 23. The present work, therefore, complements the J-resolved experiments from Ref. 23.

The present article (Part I) will be followed by an investigation of rotational influences on linewidths in the NO_2 spectrum near to the photolysis threshold (Part II) which again provides experimental information on $k(E,J)$.[34] Part III of this series describes a detailed statistical theory for $k(E,J)$ employing classical trajectories,[31] whereas in Part IV, we compare these results with more detailed quantum-statistical adiabatic channel calculations.[32]

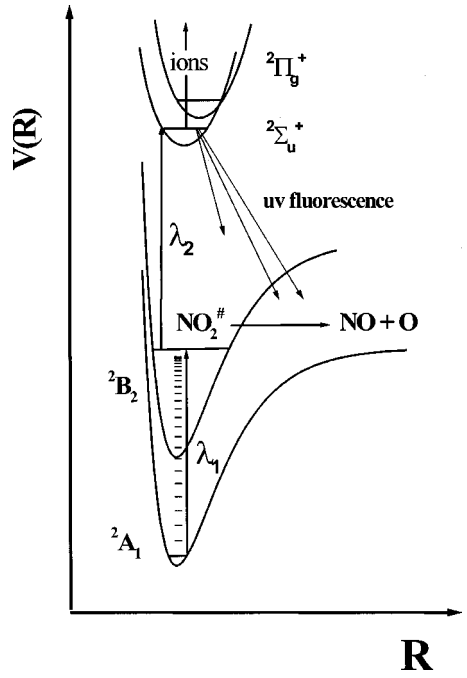

FIG. 1. Pump-and-probe level scheme of the present experiments. The excited-state dynamics can be probed via laser-induced fluorescence and ion detection.

II. EXPERIMENTAL TECHNIQUE

A. Pump-and-probe level scheme

The level scheme of our pump-and-probe experiments is illustrated in Fig. 1. The pump pulse excites either jet-cooled molecules or molecules from a thermal ensemble in a static cell at 300 K, to states slightly below, slightly above, or far above the dissociation threshold. With this one-photon excitation, mixed states are accessible which are a composition of two zeroth order excited doublet states of $^2A_1$, and $^2B_2$ electronic symmetry, which result from the well known conical intersection of the corresponding electronic surfaces.[18,42–47] After the molecules have been excited above their dissociation threshold, they dissociate and form the products $NO(^2\Pi_\Omega)$ and $O(^3P_j)$.

In contrast to the detection of the formation of NO,[19–23] we detect the parent molecule by probing highly excited NO_2 such as explained by Fig. 1. We use a near UV-laser pulse at 310 nm which further excites the molecules from the initially reached energy to the $^2\Pi_g^+$ and $^2\Sigma_u^+$ Rydberg states near to 54 000–56 000 cm^{-1}. We finally detect laser-induced fluorescence from these Rydberg states at wavelengths below 320 nm. The properties of these emitting states have been investigated in Refs. 48 and 49. Although only ionization was reported there, we also detected fluorescence from these states in the UV spectral range. The observed fluorescence allowed us to monitor the excited-state population of NO_2 during the experiment. In one experiment reported here (see Sec. III, 310 nm excitation) laser-induced ionization of excited NO_2 was detected in a small quadrupole mass spec-

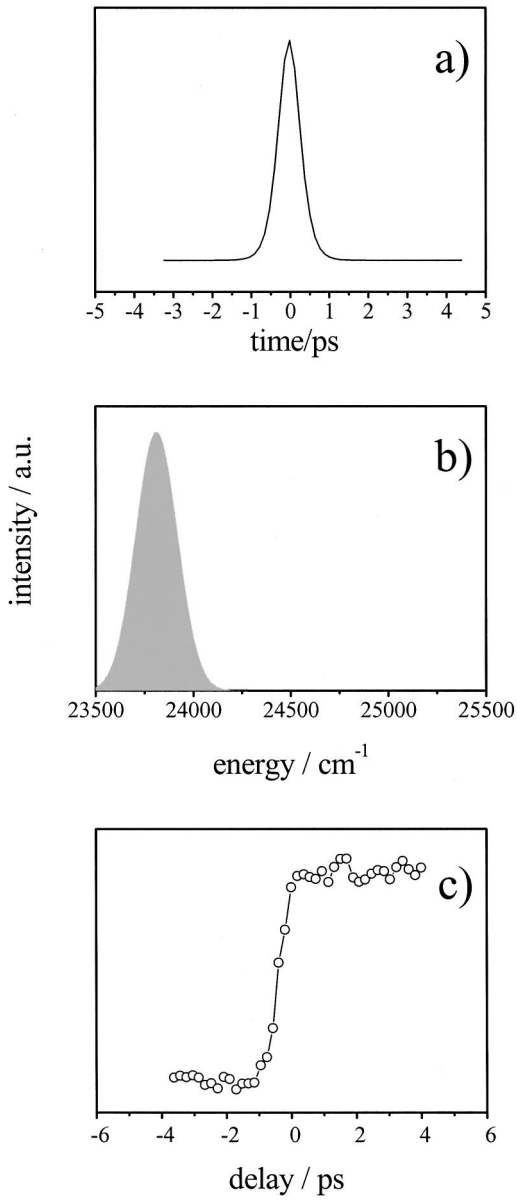

FIG. 2. Characterization of the pump-and-probe pulses. a) (Fitted) Cross-correlation which shows the time resolution of the system. b) Fitted envelope of the spectrum of the excitation pulse. c) Laser-induced fluorescence of NO_2 as a function of the delay between pump-and-probe laser pulses (pump pulses at 420 nm prepare molecules below the dissociation threshold; probe pulses at 310 nm induce the fluorescence). This trace represents the ''experimental'' integral of the experimental cross-correlation in Fig. 2(a).

trometer, attached to the vacuum chamber. Such experiments will be described elsewhere. In the given scheme, molecules also can be detected which do not dissociate; if the wavelength of the pump laser is tuned to values, where molecules are excited to energies below the dissociation threshold, a signal is recorded which does not decay. This corresponds to the situation and experimental conditions illustrated in Fig. 2: The cross-correlation of the pump and probe pulses is displayed in Fig. 2(a) whereas the spectral width of the excitation pulse is shown in Fig. 2(b). An experiment using a 420 nm-pump and 310 nm-probe pulse is shown in Fig. 2(c). The Franck–Condon factors for the pumped and probed states have been found to be similar over a broad range of wavelengths. One has to ask whether the same states are probed as reached by the pump pulse. It is known that laser pulses can coherently excite zeroth order bright states which are not eigenstates but time-dependent linear combinations of eigenstates of the molecule. In NO_2 the situation is particularly complex because mixing of the $^2B_2$ and $^2A_{1-}$ electronic states[43–46] precedes intramolecular vibrational energy redistribution (IVR). However, it is also known that the time of mixing of the $^2B_2$-state with the highly vibrationally excited $^2A_1$ ground state in NO_2 is well below 100 fs such that the time scale for state mixing and IVR in our experiments can be expected to always be below the cross-correlation time of the two laser pulses and, thus, the time resolution of the laser system. During the excitation pulse, therefore, coupling of the zeroth order electronic states and IVR can be considered to be complete such that quasieigenstates of the molecule are populated and subsequently probed. The dependence of the signals on the laser power has been controlled in all experiments in order to avoid multiphoton processes. In all cases the measured signals depended linearly on the energy of the pump and of the probe laser pulses. The time resolution of the system was found to depend strongly on the excitation wavelength. It varied between 180 and 650 fs cross-correlation times. Most of our measurements were performed with a time resolution of about 600 fs, which was found to be sufficient for measurements at excitation energies up to 1000 cm^{-1} above the dissociation threshold where NO_2 lifetimes are longer than 1 ps.

B. Experimental setup

The used experimental setup is presented schematically in Fig. 3. The required light pulses were generated by a laser system employing an argon–ion laser (Lexel 3800-8)-pumped colliding-pulse mode-locked dye laser system. Its output pulses at a wavelength of 620 nm were amplified at 20 Hz in a three stage dye amplifier which was pumped by a frequency-doubled injection-seeded Nd:YAG laser (532 nm, 60 mJ, Continuum 8020). The details of this amplifier have been described in Ref. 50. After recompression, the pulse width was less than 100 fs at energies of about 100–200 μJ, pulse intensity fluctuations were about 5%. The pulses were split into two parts of equal energy. One beam was focused into a 0.3 mm type I KDP crystal with a lens of 500 mm focal length generating frequency-doubled laser pulses at the probe wavelength 310 nm. Typical pulse energies were 15 μJ. The other beam was focused into a 1 cm water cell generating a white light continuum. By means of interference filters (bandwidth $\approx$5 nm) the desired pump wavelength at 370–420 nm was selected and subsequently amplified in a three-stage dye amplifier which was transversely pumped by the third harmonics of the Nd:YAG laser (355 nm, 50 mJ); pulse energies of 30–50 μJ with fluctuations of 15% were generated. During the experiment the cross-correlation and the zero delay could be measured via difference frequency generation in a thin BBO crystal [Fig. 2(a)]; the spectra of the pump and probe pulses were recorded routinely with a spectrograph equipped with a CCD array detector. The mea-

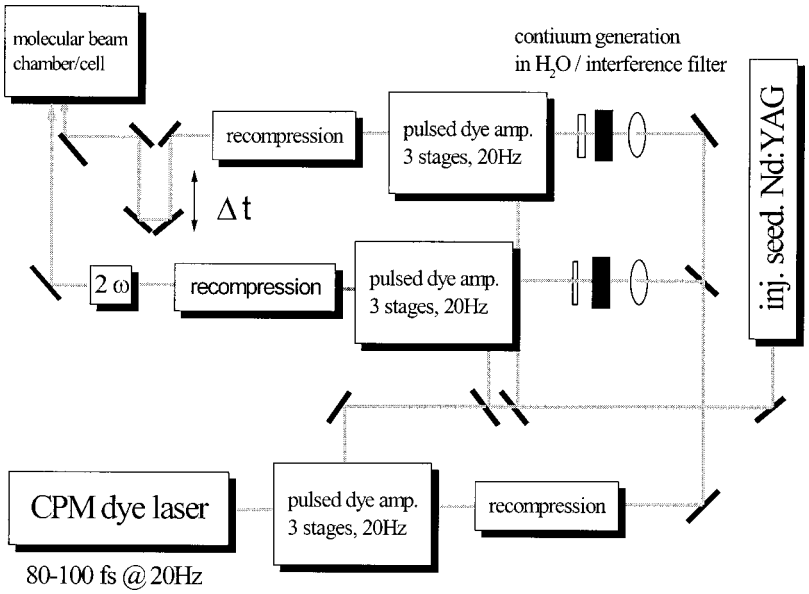

FIG. 3. Schematic experimental set up.

sured spectral width for the employed pulses typically was 210 cm^{-1} (FWHM) which is slightly larger than the Fourier limit for 600 fs laser pulses.

After passing a computer-controlled delay stage, the pump pulses were focused by a quartz lens of 350 mm focal length into a vacuum chamber. The probe pulses were independently focused with a 200 mm quartz lens. Finally, the pump and probe pulses were combined with a dichroic mirror such that they overlapped in the central part of the thermal reaction cell on the vacuum chamber containing the jet. The vacuum chamber was equipped with a pulsed nozzle of 400 μm diameter (General Valve, IOTA I) and a LIF f1.2 optics collecting the fluorescence light with a monochromator/solar blind photomultiplier tube combination (Hamamatsu, R166). Mixtures of 1–3% NO_2 in argon with stagnation pressures between 1 and 2 bar and background pressures around 10^{-4} mbar were used in the free jet expansion experiments. The expansion conditions could be varied to produce NO_2 molecules with rotational temperatures between 2 and 70 K such as determined by additional LIF experiments employing high resolution lasers. Alternatively, a small vacuum chamber was filled with about 1 mbar of NO_2 at room temperature. Whereas at 2 K only the two lowest 2 rotational levels of the NO_2 vibrational ground state are noticeably populated, at 300 K a broad distribution with $\langle J\rangle \approx 20$ is present. The population of the first excited vibrational level at room temperature is only small. Fluorescence signals from the photomultiplier were integrated, digitized (Data-Translation, DT2821-G-16SE), and processed with a personal computer. Pump- and probe-laser energies were always recorded.

III. RESULTS AND DISCUSSION

In time-resolved experiments employing ultra-short laser pulses, NO_2 dissociation can be followed directly in the time domain. A principal drawback is, however, that short light pulses have spectral widths which cover large numbers of decaying resonances (see Sec. III A and Ref. 33). The lifetime fluctuations of these resonances can give rise to nonexponential time profiles of the detected signals. These can only be analyzed by convoluting theoretically calculated lifetime distributions with the experimental pump- and probe-properties. Agreement between measured and simulated signals then is taken as an indication for the correctness of the analysis. We have succeeded to provide this internally consistent analysis for jet-cooled NO_2 near 2 K in Ref. 33. In the following, we use these low temperature experiments as a reference for comparison with our present experiments at higher rotational temperatures and with the low temperature experiments from Refs. 20 and 22.

Besides the nonexponentialities arising from lifetime fluctuations, broader rotational and energy distributions may also add contributions to nonexponential time-profiles of the observed signals, because the specific rate constants $k(E,J)$ markedly depend on the energy *E and* the angular momentum (quantum number *J*). The variations of the time-resolved traces as a function of average angular momentum is the topic of the present article. It would be desirable to measure and to resolve $k(E,J)$ directly. Due to the bandwidth of our ultrashort laser pulses and the broad excited-state distributions, in this type of experiment we obtain signals that represent complicated convolutions of individual resonance decays (in the quantum mechanical picture) or rate constants $k(E,J)$ (in the language of statistical theories). However, a deconvolution is, in any case, not feasible. Instead, theoretical $k(E,J)$ have to be generated, convoluted with the lifetime distributions as well as with the rotational distributions and the experimental resolution, before the simulated signal can finally be compared with experimental signal. The agreement between experiment and simulation then provides evidence for the correctness of the employed ''theoretical'' $k(E,J)$. Note, even a correctly averaged rate constant has to be derived this way (see Sec. III C). While lifetime fluctuations were theoretically derived from quantum mechanical calculations for $J=0$ in Ref. 33, similar quantum mechanical calculations are not yet available for larger *J*. However, the

calculations for $J=0$ on average were shown to coincide reasonably well with statistical theory. Therefore, statistical theory is used to calculate the dependence of $k(E,J)$ on E and J and to predict rotational effects. The comparison with the results from Sec. III B and III C then controls the predictions of statistical theory.

A. Reference experiments near 2 K

In Ref. 33 we have compared photodissociation experiments of jet-cooled NO_2 molecules at about 2 K with quantum mechanical calculations for $J=0$ which were based on a global *ab initio* potential energy surface. In the present article we use these data as a reference for comparison with time-resolved experiments in which broader rotational distributions have been investigated. Before looking at our experiments with broader *J*-distributions, we note that the experimental data at about 2 K not only match the quantum mechanical calculations from Ref. 33, but are also consistent with data from Refs. 20 and 22. In order to make this point clearer, we take the distribution of resonances from Ref. 33 and *predict "experimental" population-time profiles* $S(t)$ via the relation

$$S(t)=\sum_n |A_n|^2 \cdot \exp(-\Gamma_n t/\hbar), \tag{1}$$

with

$$|A_n|^2=|a_n|^2\exp(-\alpha(\overline{E}-E_n)^2), \tag{2}$$

which accounts for the spectral widths of the laser pulse ($\overline{E}$ is the center wavelength, α is related to the bandwidth of the laser pulse, Γ_n is the width of the resonance n, and a_n is related to the intensity of the transitions which was assumed to be equal for all states) and the vibrational Franck–Condon (FC) factors. Since we very likely approach saturation in the excitation step the assumption of equal FC-factors appears to be justified. In addition, we have studied the impact of this approximation and found that (random) variations in the A_n-coefficients with the correct average value did not significantly degrade the fit as long as the variations were not too large. Finally, the theoretical decay curves have been convoluted with the time resolution of the experimental system which is characterized by the normalized cross-correlation function of the two laser pulses

$$\tilde{S}(t)/\tilde{S}(t)_{\max}=\int_0^\infty S(\tau)\exp[-\delta(t-\tau)^2]d\tau. \tag{3}$$

The Gaussian in Eq. (3) is fitted to the cross-correlation function of the particular experiment. With this procedure time profiles are generated *without adjustable* parameters. A comparison of a theoretical prediction and our present experimental results for two excitation wavelengths 398 and 396 nm is shown in Fig. 4. The agreement between experiment and theory is very good. With the same procedure *"experimental"* results with quite different time resolutions and laser parameters *for* NO_2 *decay as well as for* NO-*formation* [replacing $\exp(-\Gamma_n t/\hbar)$ by $1-\exp(-\Gamma_n t/\hbar)$ in Eq. 1] can be predicted. We demonstrate the latter for two experiments from Refs. 20 and 22 [Fig. 2(b) of Ref. 22 and Fig. 4(c) of Ref. 20]. In these experiments the formation of NO after near UV excitation (380–400 nm) has been monitored with picosecond time resolution by Wittig *et al.* For these experimental conditions, we used Eqs. (1–3), added white noise to the simulation, which is proportional to the signal amplitude, and *simulated* NO-formation for these experiments. Figure 5 gives the results. The upper panel corresponds to an average excess energy of about 18 cm^{-1} (rotational quantum number $N'=1$), a laser pulse bandwidth of $\Delta\nu=30\,cm^{-1}$, and a laser pulse length of 1.6 ps (FWHM). The bandwidth of the laser pulse and the distribution of resonances are shown in the insert of Fig. 5(a). The full line (——) in Fig. 5 is a single exponential fit to the simulated data points (○). The fitted single-exponential rise time of $\tau=5$ ps is in excellent agreement with the results from the fit of the experimental data given in Ref. 22. A simulation (○) and a single exponential fit (——) for a higher excitation energy is given in Fig. 5(b) [to be compared with Fig. 4(c) of Ref. 20] corresponding to an excitation wavelength of 396.54 nm, a laser pulse bandwidth of $\Delta\lambda=0.5$ nm, and a pulse length of 1.4 ps. Our fitted single-exponential rise time of 3.5 ps to the modeled (predicted) NO-signal (○) again is in excellent agreement with the fit to the experimental data in Ref. 20. This procedure shows that the experiments from Wittig's and our laboratories are consistent and agree quantitatively with the quantum

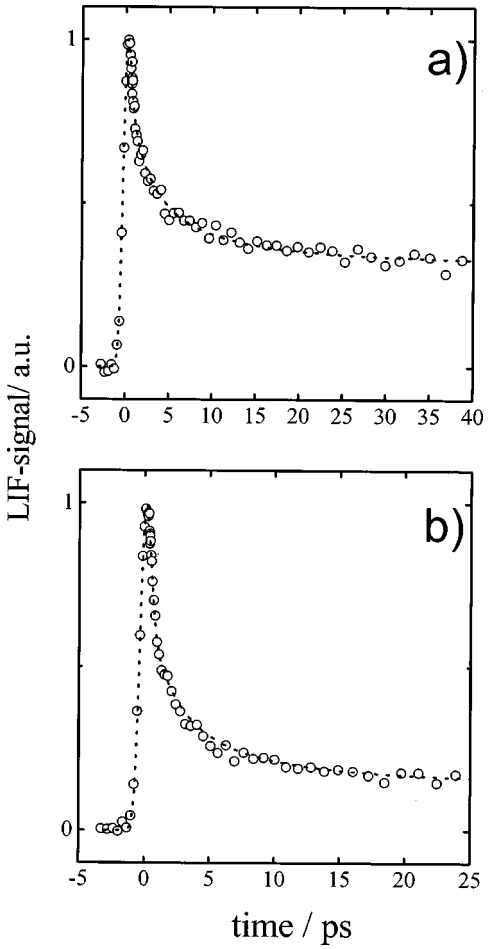

FIG. 4. a) LIF signal of NO_2 after excitation at 398 nm ($T\approx 2$ K, open circles=experimental points; dashed line: Simulation with convolution of lifetime distribution and experimental resolution, see text). b) As a) but with excitation at 396 nm.

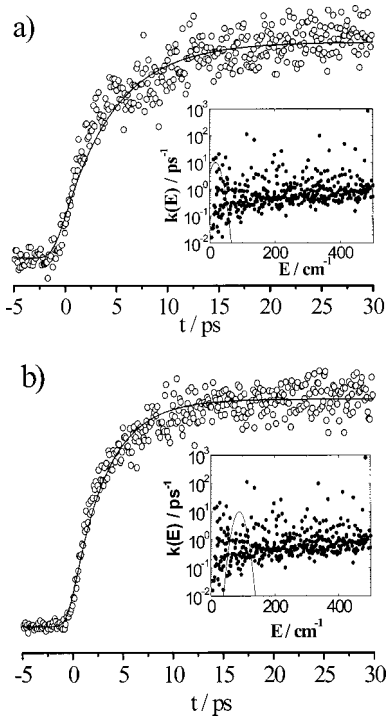

FIG. 5. Simulation (○) of NO formation in NO_2 photolysis for the experimental conditions given in Ref. 20, 22 and single exponential fit (——) to the simulation. Upper trace: 18 cm^{-1} in excess of the dissociation energy E_0; lower trace: 87 cm^{-1} in excess of E_0. Inserts: Calculated fluctuating rate constants (full circles) from Ref. 33 and spectral distributions of the excitation pulses.[20,22] For details of the simulation, see text.

mechanical calculations from Ref. 33. However, the nonexponential character of the time profiles, which is due to the marked lifetime fluctuations shown in the inserts of Fig. 5, is obviously detected more easily in our NO_2 profiles than this is possible in Wittig's NO signals.

B. Experiments at 65 and 300 K with constant excitation wavelengths

In this section, experiments at constant excitation wavelength are reported for rotational distributions corresponding to 65 and 300 K and compared with those for 2 K. The rotational temperature in the jet experiments was determined spectroscopically via standard LIF of jet-cooled NO_2 in the spectral range near to 585 nm such as elaborated in Ref. 51 Rotational energy distributions are compared with the spectral distribution of the excitation laser in Fig. 6. The shown rotational distributions and the excitation laser bandwidth (causing a significant energy distribution of the reacting molecules) have to be further convoluted with *k(E,J)* from Ref. 31 when a comparison with experiments is made. Figure 7 shows experimental signals at three different excitation wavelengths and three temperatures, namely 2 K, 65 K with $\langle E\rangle \approx 68\,cm^{-1}(J_{max}\approx 6,\langle J\rangle \approx 9)$ and 300 K with $\langle E\rangle = 313\,cm^{-1}(J_{max}\approx 15,\langle J\rangle = 20)$. Figure 7 indicates that the time profile does not change significantly when the total energy is increased by increasing rotational energy. However, near to threshold the fraction of nondissociating molecules decreases with increasing rotational energy. At shorter wavelengths, when practically all molecules dissociate [signal of Fig. 7(c)], the time dependence does not show a major influence of rotational energy. This agrees with the observations from Wittig's group.[20,22,23]

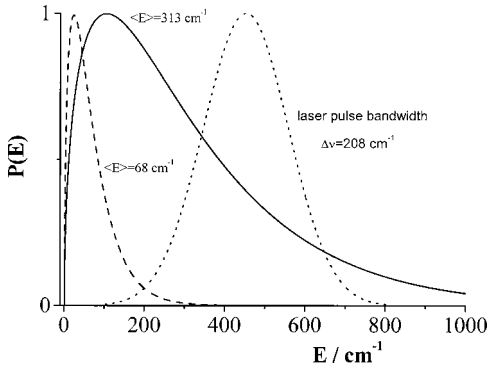

FIG. 6. Rotational distributions of NO_2 at 65 K ($\langle E\rangle = 68\,cm^{-1}$) and at 300 K ($\langle E\rangle = 313\,cm^{-1}$), respectively, which have been normalized to their maximum amplitude for clarity (not to const. area). Also shown is the spectral band width of the laser pulse used in the present experiments. See the text for more details.

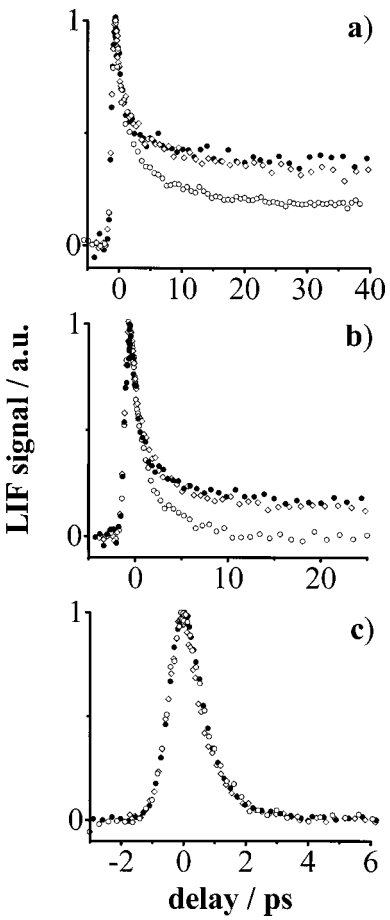

FIG. 7. LIF signals from NO_2 for various excitation conditions. a) Excitation at 398 nm; NO_2 temperatures: 2 K (filled circles), 65 K (open diamonds), and 300 K (open circles). b) Excitation at 396 nm; NO_2 temperatures: 2 K (filled circles), 65 K (open diamonds), and 300 K (open circles). c) Excitation at 383 nm; NO_2 temperatures: 2 K (filled circles), 65 K (open diamonds), and 300 K (open circles).

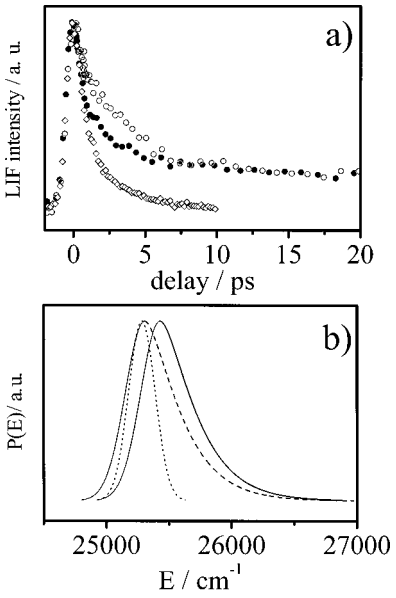

FIG. 8. LIF signals from NO_2 after various excitations. a) Excitation at 398 nm and $T=300$ K (open circles); excitation at 396 nm and $T=2$ K (filled circles); excitation at 396 nm and $T=300$ K (open diamonds) with average energies of 25 438, 25 253, and 25 565 cm^{-1}, respectively. b) Energy distributions corresponding to the three experiments form a). Note, for clarity the distributions have been normalized to their maximum amplitude and not to constant area. See the text for further details.

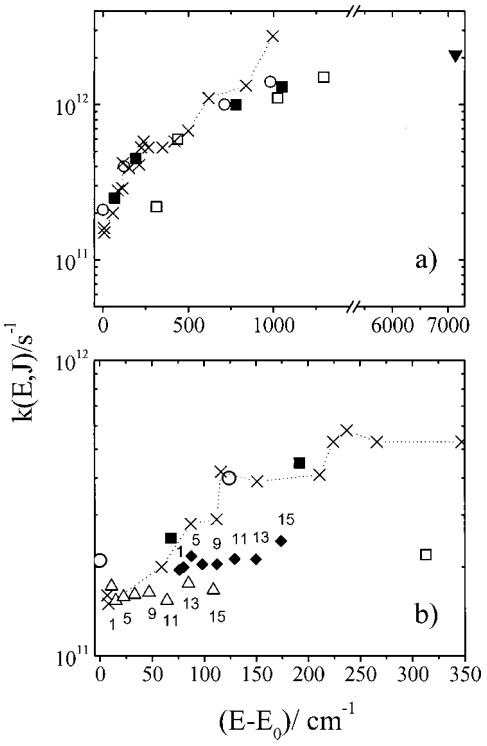

FIG. 9. Specific rate constants $k(E,J)$ for NO_2 dissociation. ○:$\langle J\rangle\approx 0$; ■:$\langle J\rangle\approx 10$; □: $\langle J\rangle\approx 20$; ▼: High energy decomposition $k(E)$ for rotationally cold $NO_2(T\approx 2$ K) for excitation at 310 nm (this work). ···×···: Rate coefficients for jet-cooled NO_2 from Ref. 20 △: Rotationally resolved rate constants with $E=10\,cm^{-1}+BN(N+1)$ from Ref. 23. ◆: Rotationally resolved rate constants with $E=75\,cm^{-1}+BN(N+1)$ from Ref. 23. E represents the sum of the vibrational and rotational energy of the reacting NO_2 molecules, averaged over the experimental distribution of excited states. Numbers in the plot are experimentally resolved J-values for data from Ref. 23: a) Larger excitation energies. b) Smaller excitation energies.

C. Experiments with variable excitation wavelengths and rotational temperatures

Statistical unimolecular rate theory predicts that, near threshold, the specific rate constants $k(E,J)$ at constant total energy E decrease with increasing J.[6] By varying excitation wavelength and rotational temperature independently, in principle, this effect could be tested exactly. For experimental reasons, we did not succeed completely to realize this test, but the set of experiments in Fig. 8 is able to show the effects of rotational excitation for sufficiently high J. In Fig. 8 we compare experiments at 398 nm with an average rotational energy of 312 cm^{-1}, at 396 nm without rotational energy, and at 396 nm with 312 cm^{-1} of rotational energy, i.e., with average total energies of 25 438, 25 253, and 25 565 cm^{-1}, respectively. Although the energy $E=25\,438\,cm^{-1}$ of the 398 nm/300K experiment is larger than the energy $E=25\,253\,cm^{-1}$ of the 396 nm/2K experiment, the decay is markedly slower. This effect is (qualitatively) in line with statistical predictions, see below. One should note that the fraction of nondissociative molecules accidentally is the same for the 396 nm/2K and 398 nm/300K experiments, because the broad spectral width of the 396 nm pulse also covers wavelengths larger than the threshold wavelengths near 398 nm.

As emphasized above, the experimental results cannot be deconvoluted to derive $k(E,J)$ directly. Instead, on the basis of a given $k(E,J)$ (here taken from Ref. 31), the convoluted experimental signal is repeatedly simulated with different global amplitudes of the parametrized $k(E,J)$ curves and compared with the experimental data. The nonreactive part of the time-resolved traces (offset) can be accounted for by assigning infinite lifetimes to the states below $E_0(J)$. Then a single averaged number $\langle k(E,J)\rangle$ is derived which can be compared with the statistical results on an *ab initio* potential energy surface without employing any adjustable parameter.[31] This appears to be the only way to obtain correctly averaged rate constants from multiexponential decays. Figure 9(a) shows the results of this procedure, i.e., $\langle k(E,J)\rangle$ as a function of $E-E_0$. In Fig. 9(a) we have plotted our average rate constants for $\langle J\rangle\approx 0$, $\langle J\rangle\approx 10$, and $\langle J\rangle\approx 20$ and a $k\ (E)$ for rotationally cold $NO_2(T\sim 2$ K, this work) for excitation at 310 nm. The data for $\langle J\rangle\approx 0$ agree quite well, in general, with the data of Wittig and co-workers. Their published data, also shown in Fig. 9(a) may suggest a rapid increase of $k\ (E)$ at higher energies. Our measured rate of $2-3\times 10^{12}\,s^{-1}$ at about 7800 cm^{-1} excess energy shows, however, that the rate constant gradually approaches a "saturation limit" for high excess energies E. If we compare the results for $\langle J\rangle\approx 0$ with those for $\langle J\rangle\gg 0$ from our study, we conclude that rotating molecules with the same total internal energy $\langle E\rangle$ decompose more slowly than nonrotating molecules. For the range of average $\langle J\rangle$- values covered in this work ($\langle J\rangle\approx 0$, $\langle J\rangle\approx 10$, $\langle J\rangle\approx 20$), this effect appears to be most pronounced for the highest average $\langle J\rangle$-values ($\langle J\rangle\approx 20$) at low excess energies where the ratio of $\langle k(E,J\approx 0)\rangle$ over $\langle k(E,J>0)\rangle$ is larger than two. It is impressive, that for our relatively broad excited-state distributions, this

effect is not averaged out. However, we do not see large differences [between $\langle k(E,J\approx 0)\rangle$ and $\langle k(E,J>0)\rangle$] at larger excess energies anymore. Also, there appears to be no large difference between the average rate constants for $\langle J\rangle \approx 10$ as opposed to $\langle J\rangle \approx 0$ at all energies (at constant total internal energy $\langle E\rangle$).

The representation of Fig. 9 also contains *J*-resolved results from Refs. 20 and 23. In the following, we will show that these data, when plotted in the way of Fig. 9, follow the same trends as found in the present work. In addition to the data from this work, Fig. 9(b) contains rotationally resolved data from Ref. 23, from two vibrational progressions for which the excess energy is $\langle E\rangle - D_0 = 10\,\mathrm{cm}^{-1} + E_{\mathrm{rot}}(101)$ and $\langle E\rangle - D_0 = 75\,\mathrm{cm}^{-1} + E_{\mathrm{rot}}(101)$ [D_0 denotes the dissociation energy for $J=0$ and $E_{\mathrm{rot}}(101)$ the rotational energy of the intermediate 101 combination vibration] and data for $J\sim 0$. Looking at the values of the *J*-resolved data alone, one may be tempted to conclude that there is no effect on the specific rate constant when changing *J*. However, when comparing rate constants for $J>0$ and for $J\sim 0$ in Fig. 9(b) a pronounced deviation of the two sets of data with increasing *J* is obvious and clearly visible. Under isoenergetic conditions, i.e., for constant E_{tot} here, the rates for $J\sim 0$ and $J>0$ appear to deviate for larger rotational excitation. Apparently, the rates for rotating molecules remain below the rates for nonrotating molecules with $J\sim 0$. This is clearly observable for $N=11-15$ in Fig. 9(b). It is interesting to note that the ratio of the rates for $J\sim 0$ and $N=15$ (e.g., in the $\langle E\rangle - D_0 = 75\,\mathrm{cm}^{-1} + E_{\mathrm{rot}}(101)$ progression) is about a factor of two. Our experiments with $\langle J\rangle = 20$ and $J_{\max}=16$ actually seem to complement these data and appear to be consistent with them. In contrast to the conclusions of Ref. 23, we conclude that for higher *J* the experimental findings may be consistent with predictions from statistical theory. However, at the same time Fig. 9(b) also shows, that for constant total energy *E*, the rates for lower angular momentum *N* are very close to $k(\langle E\rangle, J\sim 0)$ and show no large dependence on *N*. At this stage it is difficult to speculate about possible reasons for this behavior. Wittig *et al.* have attributed this effect to incomplete *K*-mixing and a pronounced role of intramolecular Coriolis coupling for the low *J* decomposition of the molecule.[23]

A somewhat surprising experimental result of the studies from Ref. 23 is that specific rate constants with $N=1$, belonging to two vibrational progressions with vibrational excess energies of 10 and 75 cm^{-1}, are about the same for low *J*. This result is correlated with the energy dependence of specific rate constants rather than its rotational dependence. If confirmed experimentally, this observation may indicate that rate fluctuations for different *J* around an average are significant and may compensate the energy dependence of $k(E,J)$ in this particular case.

IV. CONCLUSIONS

We have demonstrated that the rotational dependence of specific rate constants $k(E,J)$ of unimolecular bond fission reactions not only can be monitored in *J*-resolving experiments, but also by comparing experiments with different, well-defined thermal rotational distributions. Detecting the disappearing molecules instead of the forming products, nonexponential time profiles become manifest. In the presence of lifetime fluctuations, broad spectral distributions from the excitation light, and of broad thermal rotational distributions, the deconvolution of the experimental profiles is a problem. A simulation starting from a plausible set of $k(E,J)$ calculations with subsequent convolutions and comparison with the experiments then provides the logical approach.

By studying broader distributions, we obtained a series of results which are consistent with the *J*-resolved results from Wittig and co-workers.[20,22,23] We could demonstrate that, at a given total energy *E*, the measured $k(E,J)$ decrease with increasing *J*. This is in line with predictions form statistical unimolecular rate theory. A more quantitative theoretical analysis of the *J*-dependence is given in Part III of this series.[31] This analysis also demonstrates that the apparent lack of a rotational influence on $k(E,J)$ observed in Refs. 22 and 23 can be, at least in part, due to the compensation of two effects, i.e., the increase of $k(E,J)$ for a given *J* with increasing total *E* and the decrease of $k(E,J)$ for a given total *E* with increasing *J*. As shown in Part III, the statistical theory in this way explains the results from Refs. 22 and 23 for $J>10$ (see data in Fig. 9). However, it does not account for results at smaller *J* near to threshold (see the discussion in Ref. 31).

ACKNOWLEDGMENTS

The authors enjoyed stimulating discussions of this work with R. Schinke, S. Grebenshchikov, V. Ushakov, A. Maergoiz, and C. Wittig. Financial support from the Deutsche Forschungsgemeinschaft (SFB 357 ''Molekulare Mechanismen Unimolekularer Prozesse'') is gratefully acknowledged. The authors also thank G. Thurau for valuable assistance with the experimental set up.

[1] J. Troe, Ber. Bunsenges. Phys. Chem. **73**, 144 (1969).
[2] J. Troe, Ber. Bunsenges. Phys. Chem. **73**, 906 (1969).
[3] H. Gaedke and J. Troe, Z. Naturforsch. A **25A**, 789 (1970).
[4] H. Gaedke and J. Troe, Ber. Bunsenges. Phys. Chem. **79**, 184 (1975).
[5] H. Gaedke, H. Hippler, and J. Troe, Chem. Phys. Lett. **16**, 177 (1972).
[6] M. Quack and J. Troe, Ber. Bunsenges. Phys. Chem. **78**, 240 (1974).
[7] G. E. Busch and K. R. Wilson, J. Chem. Phys. **56**, 3638 (1972).
[8] G. E. Busch and K. R. Wilson, J. Chem. Phys. **56**, 3655 (1972).
[9] M. Quack and J. Troe, Ber. Bunsenges. Phys. Chem. **79**, 469 (1975).
[10] M. Mons and I. Dimicoli, Chem. Phys. **130**, 307 (1989).
[11] S. Reid and H. Reisler, J. Phys. Chem. **100**, 474 (1996).
[12] S. A. Reid and H. Reisler, J. Chem. Phys. **101**, 5683 (1994).
[13] J. Miyawaki, K. Yamanouchi, and S. Tsuchiya, J. Chem. Phys. **99**, 254 (1993).
[14] U. Robra, H. Zacharias, and K. H. Welge, Z. Phys. D: At., Mol. Clusters **16**, 175 (1990).
[15] J. A. Mueller, S. A. Rogers, and P. L. Houston, J. Phys. Chem. A **102**, 9666 (1998).
[16] T. J. Butenhoff and E. A. Rohlfing, J. Chem. Phys. **98**, 5469 (1993).
[17] T. J. Butenhoff and E. A. Rohlfing, J. Chem. Phys. **98**, 5460 (1993).
[18] B. Abel, H. H. Hamann, and N. Lange, Faraday Discuss. **102**, 147 (1995).
[19] I. Bezel, D. Stolyarov, and C. Wittig, J. Phys. Chem. **103**, 10268 (1999).
[20] S. I. Ionov, G. A. Bruckner, C. Jaques, Y. Chen, and C. Wittig, J. Chem. Phys. **99**, 3420 (1993).
[21] S. I. Ionov, H. F. Davis, K. Mikhaiylichenko, L. Valachovic, R. A. Beaudet, and C. Wittig, J. Chem. Phys. **101**, 4809 (1994).
[22] P. I. Ionov, I. Bezel, S. I. Ionov, and C. Wittig, Chem. Phys. Lett. **272**, 257 (1997).
[23] I. Bezel, P. Ionov, and C. Wittig, J. Chem. Phys. **111**, 9267 (1999).

[24] A. V. Demyanenko, A. V. Dribinski, H. Reisler, H. Meyer, and C. X. W. Quian, J. Chem. Phys. **111**, 7383 (1999).
[25] S. Y. Grebenshchikov, C. Beck, H. Flöthmann, R. Schinke, and S. Kato, J. Chem. Phys. **111**, 619 (1999).
[26] L. B. Harding, H. Stark, J. Troe, and V. G. Ushakov, Phys. Chem. Chem. Phys. **1**, 63 (1999).
[27] S. J. Klippenstein and T. Radivoyevitch, J. Chem. Phys. **99**, 3644 (1993).
[28] R. F. Salzgeber, V. Mandelshtam, C. Schlier, and H. S. Taylor, J. Chem. Phys. **109**, 937 (1998).
[29] R. Brandi, F. Santoro, and C. Petrolongo, Chem. Phys. **225**, 55 (1997).
[30] H. Katagiri and S. Kato, J. Chem. Phys. **99**, 8805 (1993).
[31] B. Abel, J. Troe, and V. Ushakov, J. Chem. Phys. (submitted).
[32] B. Abel, A. Maergoiz, and J. Troe, J. Chem. Phys. (to be published).
[33] B. Kirmse, B. Abel, D. Schwarzer, S. Grebenshchikov, and R. Schinke, J. Chem. Phys. A **104**, 10398 (2000).
[34] B. Abel, N. Lange, and J. Troe, J. Chem. Phys. **115**, 6531 (2001), following paper.
[35] W. H. Hase, Acc. Chem. Res. **31**, 659 (1998).
[36] S. Y. Grebenshchikov, H. Flöthmann, R. Schinke, I. Bezel, C. Wittig, and S. Kato, Chem. Phys. Lett. **285**, 410 (1998).
[37] H. J. Neusser, J. Phys. Chem. **93**, 3897 (1989).
[38] F. Reiche, B. Abel, R. Beck, and T. R. Rizzo, J. Chem. Phys. **112**, 8885 (2000).
[39] A. Callegari, J. Rebstein, R. Jost, and T. R. Rizzo, J. Chem. Phys. **111**, 7359 (1999).
[40] C. M. Roehl, J. J. Orlando, G. S. Tyndall, R. E. Shetter, G. J. Vazquez, C. A. Cantrell, and J. G. Calvert, J. Phys. Chem. **98**, (1994).
[41] J. N. Pitts, J. H. Sharp, and S. I. Chan, J. Chem. Phys. **40**, 3655 (1964).
[42] D. Douglas and H. Huber, Can. J. Phys. **43**, 74 (1965).
[43] A. Delon and R. Jost, J. Chem. Phys. **95**, 5686 (1991).
[44] A. Delon, R. Jost, and M. Lombardi, J. Chem. Phys. **95**, 5701 (1991).
[45] A. Delon, R. Georges, and R. Jost, J. Chem. Phys. **103**, 7740 (1995).
[46] A. Delon, R. Jost, and M. Jacon, J. Chem. Phys. **114**, 331 (2001).
[47] J. Livien, A. Delon, and R. Jost, J. Chem. Phys. **108**, 8931 (1998).
[48] L. Bigio and E. R. Grant, J. Chem. Phys. **87**, 360 (1887).
[49] L. Bigio and E. R. Grant, J. Chem. Phys. **83**, 5361 (1985).
[50] T. Bultmann, D. Bingemann, N. P. Ernsting, D. Schwarzer, and L. Nikowa, Rev. Sci. Instrum. **66**, 4393 (1995).
[51] R. E. Smalley, L. Wharton, and D. H. Levy, J. Chem. Phys. **63**, 4977 (1975).